Chapter 6

Pharmacological Inhibition of Intracellular Signaling Pathways in Radioresistant Anaplastic Thyroid Cancer

Dmitry Bulgin and Alexey Podcheko

Additional information is available at the end of the chapter

http://dx.doi.org/10.5772/62541

Abstract

Anaplastic thyroid cancer (ATC) is highly aggressive and has a poor therapeutic response and leads to high mortality. It has been shown that activation of intracellular c-Jun N-terminal kinase (JNK) and c-ABL signaling pathways is one of the manifestations of the highly resistant response to radiotherapy in ATC. Pharmacological inhibition of these pathways in combination with radiotherapy is a potential treatment modality of ATC.

Keywords: Anaplastic thyroid cancer, JNK signaling pathway, c-ABL signaling pathway, ionizing radiation, radioresistance, anthrapyrazolone, imatinib

1. Introduction

Thyroid malignant neoplasms are the most frequent endocrine tumor. They are classified into two categories, differentiated carcinoma and undifferentiated carcinoma (anaplastic carcinoma), based on the histological differentiation (Figure 1).

In the clinical course, differentiated thyroid carcinomas such as follicular cancer and papillary cancer have relatively good prognosis. ATC is among the most aggressive solid malignancies in human with a bad prognosis. In spite of active therapeutic and surgical treatment, ATC provides mean survival time less than 8 months after diagnosis [1]. ATC is widely metastatic, and it is highly resistant to regular therapeutic approaches such as surgical treatment, chemotherapy, or radiotherapy. It was confirmed that thyroid cells are relatively resistant to ionizing radiation (IR)-induced apoptosis [2, 3].

Currently, it is mainly approved that external beam radiotherapy of ATC should be combined with different anti-tumor pharmacological agents to have better local control of the tumor [4]. The main goal of this combination is to reduce the clonogenic capacity and radioresistance of

classified into two categories, differentiated carcinoma and undifferentiated carcinoma (anaplastic carcinoma), based on the histological differentiation (Figure 1).

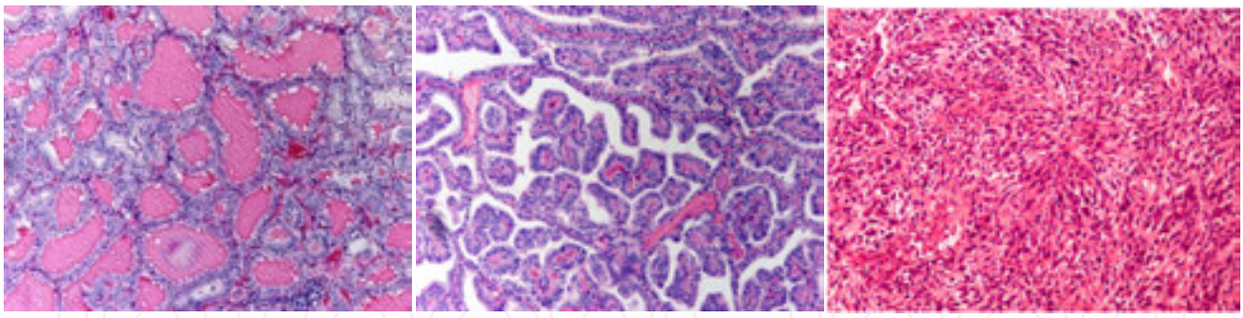

(a) (b) (c)

Figure 1. Thyroid malignant neoplasms histology: (a) follicular carcinoma; (b) papillary carcinoma; and (c) anaplastic carcinoma (courtesy of professor Masahiro Nakashima, Nagasaki University, Japan). Hematoxylin and eosin stain. Original magnification ×100.

Figure 1. Thyroid malignant neoplasms histology: (a) follicular carcinoma; (b) papillary carcinoma; and (c) anaplastic carcinoma. Hematoxylin and eosin stain. Original magnification ×100.

In the clinical course, differentiated thyroid carcinomas such as follicular cancer and papillary cancer have relatively good prognosis. Anaplastic thyroid cancer (ATC) is among the most aggressive solid malignancies in human with a bad prognosis. In spite of active therapeutic and surgical treatment, ATC provides mean survival time less than 8 months after diagnosis [1]. ATC is widely metastatic, and it is highly resistant to regular therapeutic approaches such as surgical treatment, chemotherapy, or radiotherapy. It was confirmed that thyroid cells are relatively resistant to ionizing radiation (IR)-induced apoptosis [2, 3].

Currently, it is mainly approved that external beam radiotherapy of ATC should be combined with different anti-tumor pharmacological agents to have better local control of the tumor [4]. The main goal of this combination is to reduce the clonogenic capacity and radioresistance of ATC cells with the aim of further improving the radiotherapy effect. It is conceivably that molecular-targeted pharmacological agents can decrease cancer resistance to radiotherapy through modulation of DNA repair, cell death pathway, intracellular signal transduction [5, 6], or senescence-like terminal growth arrest [7].

2. Radiation therapy

Radiation therapy, like most anti-tumor treatments, achieves its therapeutic effect by inducing different types of cell death in tumors [8]. Over the past decade, our knowledge is rapidly increasing regarding the discovery of various molecular pathways involved in determining cell death after IR exposure [9]. The biological target of IR in the cell is DNA (Figure 2).

Double-strand breaks (DSBs) are the most destructive DNA alterations, which, if left unrepaired, may have serious consequences for cell survival, as they lead to genomic instability, loss of genetic information, and cell death. DSBs are responsible for more than 70% of single-strand DNA breaks for most of cell death in tumor as well as surrounding normal cells. Cells respond to DNA damage by activating complex processes at the level of molecules and genes to detect and repair DNA alterations. The formation of DSBs activated phosphorylation of H2AX (the subtype of histone H2A). The phosphorylated form of H2AX is called γ-H2AX [10]. Phosphorylation of H2AX plays a key role in DNA reparation, and it is necessary for the assembly of DNA repair molecules at the sites containing damaged chromatin as well as for activation of checkpoint proteins, which arrest the cell cycle progression [11]. The evaluation of γ-H2AX levels may allow not only to control the efficiency of antitumor therapy but also to predict cancer cell sensitivity to DNA-damaging anti-tumor agents and toxicity of anti-tumor treatment toward normal cells. It is possible to detect H2AX phosphorylation by specific γ-H2AX antibody and thus to detect DNA damage and repair *in situ* in individual cells. The presence of γ-H2AX in chromatin can be exposed shortly after induction of DSBs in the form of discrete nuclear foci (Figure 3) [12]. The presence of γ-H2AX containing nuclear foci can be measured by microscopy, flow cytometry, and Western blotting of tissue/cell lysates [13].

http://dx.doi.org/10.5772/62541

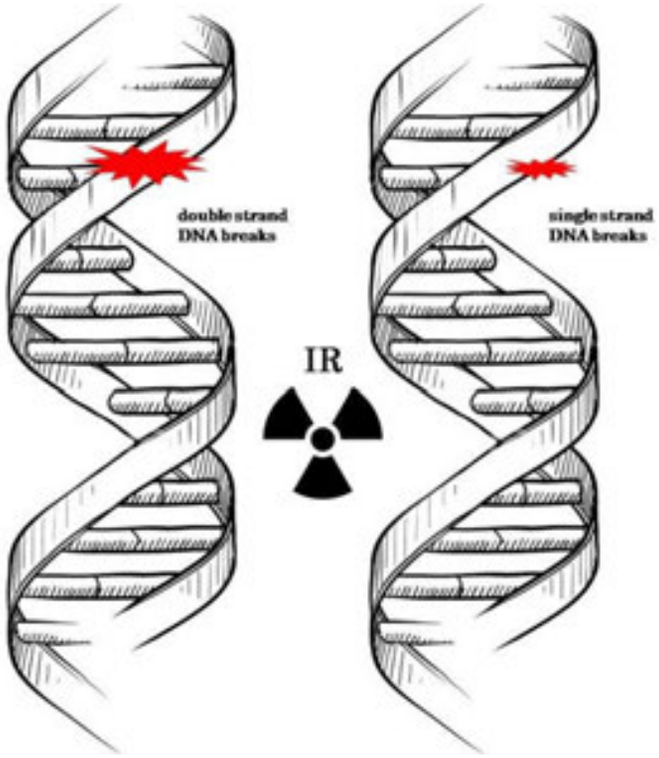

Figure 2. The biological target of IR in the cell is DNA. IR-induced DNA damage of cancer cells can lead to cell death.

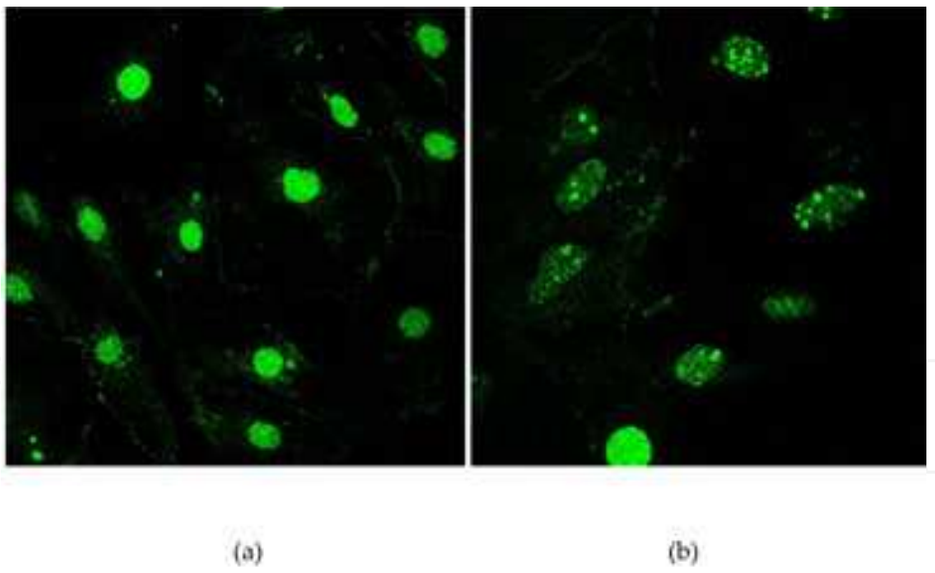

Figure 3. IR induces γ-H2AX nuclear foci formation in ATC cell lines: (a) non-radiated; (b) in 24 hours after 10 Gy IR treatment (EXS-300 X-irradiator, Toshiba, Tokyo, Japan; 200 kV, 15 mA, 0.83 Gy/min). Compared to alternative methods of DNA damage assessment, the immunocytochemical approach is less cumbersome and offers much greater sensitivity. Fluorescent immunocytochemistry. Confocal fluorescent microscopy. Original magnification ×400.

The main goal of radiotherapy is to deprive tumor cells of their multiplication potential and finally to destroy the cancer cells. After IR exposure, cell death may occur by one or more of

the following mechanisms: immediate or delayed apoptosis, mitotic-linked death (mitotic catastrophe), autophagy, and terminal growth arrest (senescence) associated with necrosis (Figure 4).

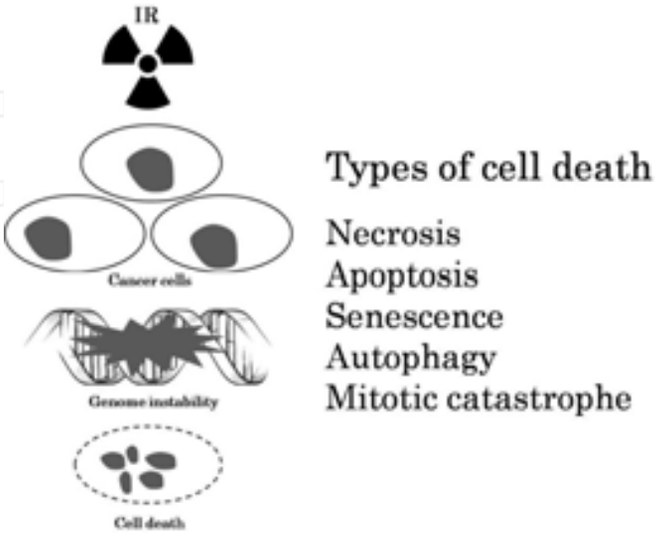

Figure 4. Mechanisms of cancer cell death triggered by IR.

Radiotherapy does not destroy cancer cells right away. It takes hours, days, or weeks of anti-tumor therapy before cancer cells start to die after which cancer cells continue dying for weeks to months after ending of radiotherapy. The efficiency of radiotherapy has much to gain by understanding the cell death mechanisms that are induced in tumor cells following irradiation (Table 1). Strategies to use specific pharmacological agents that can inhibit the activity of key molecules in intracellular signaling pathways combined with IR might potentiate therapy and enhance tumor cell death [14].

Types of cell death	Definition and characteristics	Associated changes	Detection methods
Necrosis	Cells visibly swell with breakdown of cell membrane. Typical nuclei with vacuolization and disintegrated cell organelles.	Sometimes not considered genetically determined. Drop of ATP levels. ROS over-generation.	Early permeability to vital dyes. Staining with propidium iodide. Electron microscopy.
Apoptosis	Programmed cell death. Cells shrink with blebbing of cell membranes. Condensed chromatin and DNA fragmentation.	Stimulated by cyclin D1 activation and by Myc. Can be inhibited by loss of wild-type p53. Caspase activation.	Sub-G1 peak in flow cytometry. Annexin-V staining. Quantification of $\Delta\Psi m$. Internucleosomal laddering.

http://dx.doi.org/10.5772/62541

Types of cell death	Definition and characteristics	Associated changes	Detection methods
		Dissipation of mitochondrial transmembrane potential ($\Delta\Psi m$).	
Senescence	Cells do not divide, although they remain metabolically active. Large and flat cells with increased granularity.	Stimulated by Ras mutations and telomerase shortening. Inhibited by the loss of wild-type p53, p16, and $p21^{WAF1}$.	Staining for β-galactosidase at pH 6 (SA-β-Gal+). Absence of DNA synthesis (BrdU incorporation).
Autophagy	Programmed cell death in which the cell digests itself. Formation of vacuoles in cytoplasm.	Cell death is accompanied by massive autophagic vacuolization of cytoplasm without condensation. LC3-I to LC3-II conversion (LC3, microtubule-associated protein).	Immunoblotting with LC3-specific antibodies. Immunofluorescence microscopy (LC3-GFP fusion protein).
Mitotic catastrophe	Cell death occurring during or after a faulty mitosis. Giant cells with two or more nuclei and partially condensed chromatin. Can lead to necrosis or apoptosis-like death (p53-independent).	Stimulated by deficiencies in proteins involved in G1 and G2 checkpoints and in mitotic spindle assembly. Can follow caspase-dependent or caspase-independent pathways.	Cells with two or more nuclei detected by microscopy or laser scanning cytometry. Aberrant mitotic figures. Accumulation in G2/M and polyploidy.

Table 1. Anti-proliferative response and cell death pathways observed upon radiotherapy.

3. JNK signaling pathway

c-Jun N-terminal kinases (JNKs) are multifunctional kinases, also known as stress-activated protein kinases be a part of superfamily of mitogen-activated protein kinases (MAPKs) that are involved in many physiological and pathological processes (Figure 5). At first, the JNKs were originally identified as ultraviolet-responsive protein kinases by their capacity to phosphorylate the N-terminal of the transcription factor c-Jun and by their activation in response to various stresses [15]. Initial research works have shown that JNKs can be triggered by various stimuli including growth factors [16, 17], cytokines [18], and stress factors [19]. It was demonstrated that IR with level of 10 Gy induced JNK activation with a maximum at 30 minutes and return to baseline at 12 hours after exposure in ATC cell lines [7].

Other observations have demonstrated the crucial role of JNK pathway in mediating apoptotic signaling in many cell death paradigms [20]. JNK signal transduction pathway regulates the cellular reaction to IR and activating radiation-induced apoptosis [21]. However, it was shown

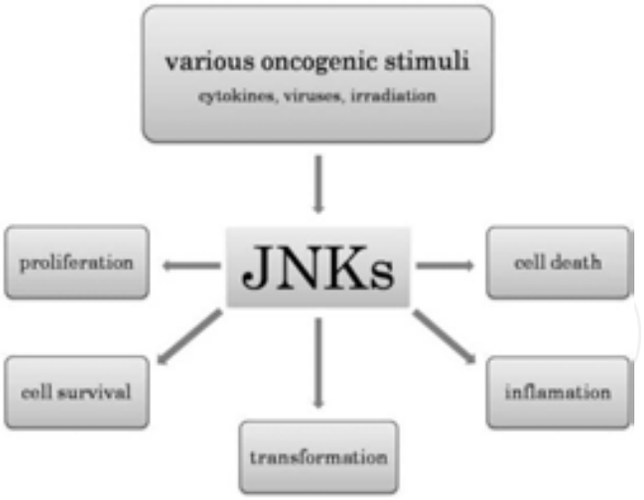

Figure 5. Various extracellular and intracellular stimuli can activate JNKs. Constant JNK activation influences tumourigenesis by both transcription-independent and transcription-dependent mechanisms involved in cell transformation, proliferation, survival, migration, suppression of cell death, and inflammatory processes in tumor.

that JNK cascade, via the stimulation of c-Jun and ATF-2 transcription factors, may provide DNA repair and cell survival (Figure 6) [22].

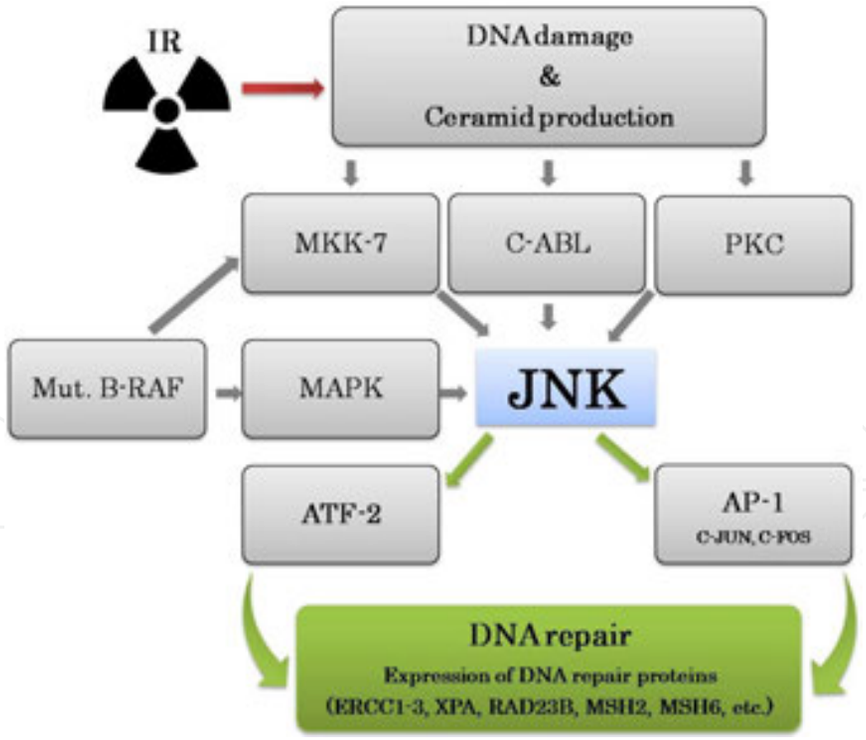

Figure 6. Role of JNK kinase in DNA repair after IR-induced extensive damage.

For that reason, it was proposed that JNK pathway inhibition could result in sensitization of distinct types of tumor cells to DNA damage.

http://dx.doi.org/10.5772/62541

c-ABL is an ubiquitously expressed tyrosine kinase that involves in various cellular signaling processes. The c-ABL is highly expressed in normal and cancer cells [23, 24].

4. c-ABL tyrosine kinase signaling pathway

c-ABL is an ubiquitously expressed tyrosine kinase that involves in various cellular signaling processes. The c-ABL is highly expressed in normal and cancer cells [23, 24].

c-ABL is frequently overexpressed in thyroid cancer tissue samples (Figure 8).

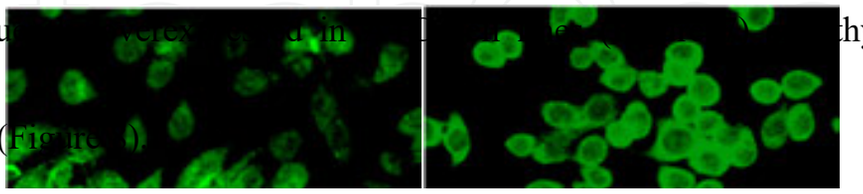

Figure 7. c-ABL expression in ATC cell lines: (a) FRO cell line and (b) ARO cell line. Fluorescent immunocytochemistry. Confocal fluorescent microscopy. Original magnification ×400.

Figure 7. c-ABL expression in ATC cell lines: (a) FRO cell line and (b) ARO cell line. Fluorescent immunocytochemistry. Confocal fluorescent microscopy. Original magnification ×400.

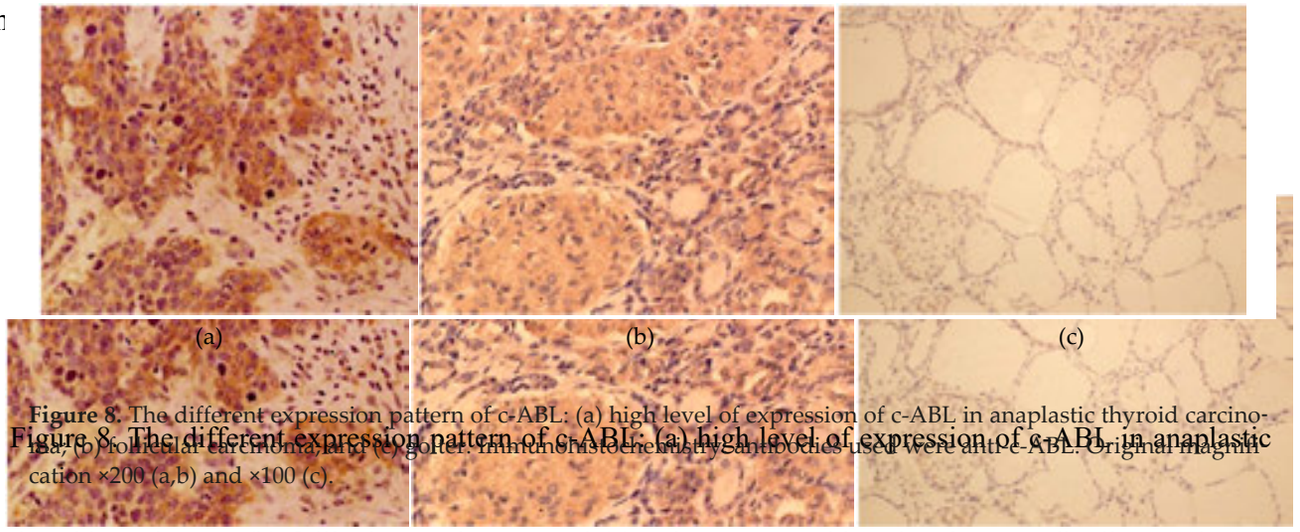

Figure 8. The different expression pattern of c-ABL: (a) high level of expression of c-ABL in anaplastic thyroid carcinoma, (b) follicular carcinoma, and (c) goiter. Immunohistochemistry. Antibodies used were anti-c-ABL. Original magnification ×200 (a,b) and ×100 (c).

Figure 8. The different expression pattern of c-ABL: (a) high level of expression of c-ABL in anaplastic thyroid carcinoma, (b) follicular carcinoma, and (c) goiter. Immunohistochemistry. Antibodies used were anti-c-ABL. Original magnification ×200 (a,b) and ×100 (c).

Previous experiments indicated that c-ABL is involved in regulation of the cell cycle and the cellular genotoxic stress response pathways. It was demonstrated that the growth arrest was accompanied by the down-regulation of c-ABL phosphorylation and of cyclins A and B1 levels and by the up-regulation of the cell cycle inhibitor $p21^{cip1}$. Also, it was presented that $p21^{cip1}$ expression is associated with improved survival in patients after adjuvant radiotherapy [25].

The cellular reactions elicited by c-ABL depends upon its location in cells. Accumulation of c-ABL in the cytoplasm results in cell survival and proliferation. By contrast, nuclear c-ABL and the cellular genotoxic stress response pathways. It was demonstrated that the growth arrest was accompanied by the down-regulation of c-ABL phosphorylation and of cyclins A and B1 levels and by the up-regulation of the cell cycle inhibitor $p21^{cip1}$.

induces apoptosis following genotoxic stress [26]. DNA damage caused by IR and other

DNA-damaging agents has been shown to result in activation of the c-ABL (Figure 9)

[27].

becomes activated and induces apoptosis following genotoxic stress [26]. DNA damage caused by IR and other DNA-damaging agents has been shown to result in activation of the c-ABL (Figure 9) [27].

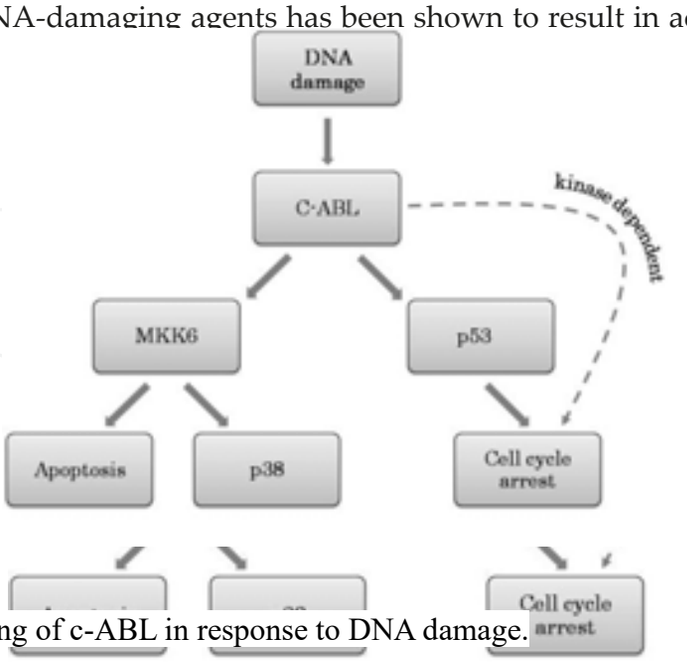

Figure 9. Nuclear targeting of c-ABL in response to DNA damage.

Figure 9. Nuclear targeting of c-ABL in response to DNA damage.

It was demonstrated that IR induces redistribution of c-ABL between nucleus and

It was demonstrated that IR induces redistribution of c-ABL between nucleus and cytoplasm in ATC cells (Figure 10) [28].

cytoplasm in ATC cells (Figure 9) [28].

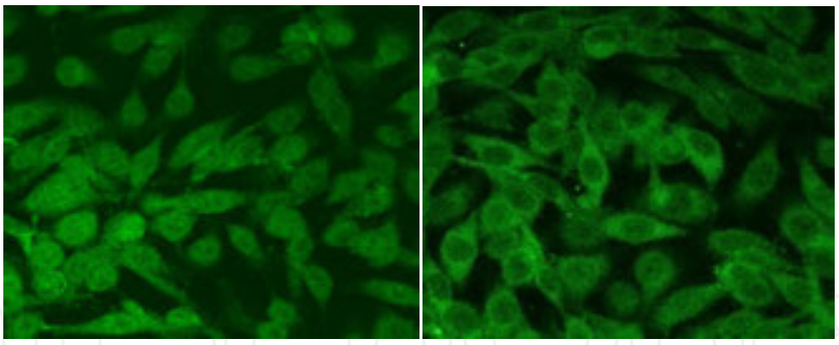

(a) (b)

Figure 10. IR induces redistribution of c-ABL between nucleus and cytoplasm in ATC cells. Translocation of c-ABL in FRO cells after IR treatment (EXS-300 X-irradiator, Toshiba, Tokyo, Japan; 200 kV, 15 mA, 0.83 Gy/min); (a) non-radiated; (b) in 6 hours after 10 Gy IR treatment. Fluorescent immunocytochemistry. Confocal fluorescent microscopy. Original magnification ×400.

Figure 10. IR induces redistribution of c-ABL between nucleus and cytoplasm in ATC cells. Translocation of c-ABL in FRO cells after IR treatment (EXS-300 X-irradiator, Toshiba, Tokyo, Japan; 200 kV, 15 mA, 0.83 Gy/min); (a) non-radiated; (b) in 6 hours after 10 Gy IR treatment. Fluorescent immunocytochemistry. Confocal fluorescent microscopy. Original magnification ×400.

Notably, nuclear targeting of c-ABL is required for the induction of apoptosis in DNA damage. Overexpression of c-ABL activates cell cycle arrest in G1, which requires kinase activity and nuclear localizing signals and depends on the wild-type p53 tumor suppressor (Figure 10). In addition, c-ABL binds p53 and enhances the DNA binding and transcriptional activity of p53 [29, 30].

http://dx.doi.org/10.5772/62541

Previous studies have revealed that loss of wild-type p53 function by mutation of the gene can lead differentiated thyroid cancer to anaplastic change [31, 32]. ATC is harbor mutations of p53 in 80–90% of cases and characterized by aggressive course of disease. It was previously demonstrated that thyroid cancer cells with p53 mutation are relatively resistant to IR-induced apoptosis [33]. Relationships between c-ABL and p53 revealed dependence of p53-deficient cells from c-ABL for enhanced proliferation, suggesting that pharmacologic inhibition of c-ABL may have therapeutic value in the p53-deficient cancer cells [34]. Hence, pharmacological inhibition of c-ABL kinase activity can modify the response of ATC cells to IR and could be a promising treatment modality.

5. Senescence-like terminal growth arrest

Senescence is a physiological process of changes in cell metabolism associated with a series of inductive, permissive, and restrictive communications that limit the cell proliferative capacity. Senescent cells are viable but non-dividing, stop to synthesize DNA, and become enlarged and flattened with an increased granularity. Recent data show that senescence may act as an acute, drug- or IR-induced growth arrest program in numerous stromal and epithelial tumors [35]. It was found that IR induces senescence-like phenotype (SLP) associated with terminal growth arrest in ATC cell lines and also in primary thyrocyte line in time- and dose-dependent manner [36].

The induction of SLP in thyroid cells can be identified by the following:

- Senescence-associated β-galactosidase (SA-β-Gal) staining method (Figure 11)
- Dual-flow cytometric analysis of cell proliferation and side light scatter using vital staining with PKH-2 dye
- Double labeling technique for SA-β-Gal and 5-bromo-2′-deoxyuridine (BrdU)
- Staining for SA-β-Gal with consequent anti-thyroglobulin immunocytochemistry (Figure 12)

6. Anthrapyrazolone as a specific inhibitor of JNK signaling pathway

Anthrapyrazolone is a synthetic polyaromatic small molecule–specific inhibitor of c-JNK signaling (Figure 13). Anthrapyrazolone acts as a reversible ATP-competitive inhibitor with an identical capability toward JNK1, JNK2, and JNK3 with >20-fold selectivity versus various tested kinases other than JNKs [37, 38].

In cell cultures, anthrapyrazolone shows dose-dependent inhibition of c-Jun phosphorylation in the range of 5–50 μM [38]. It was demonstrated that combination of anthrapyrazolone and IR treatment inhibited ATC cell growth [7]. Numerous SA-β-Gal–positive cells were markedly increased when anthrapyrazolone was combined with IR (Figure 14).

- Dual-flow cytometric analysis of cell proliferation and side light scatter using vital staining with PKH-2 dye
- Double labeling technique for SA-β-Gal and 5-bromo-2'-deoxyuridine (BrdU)
- Staining for SA-β-Gal with consequent anti-thyroglobulin immunocytochemistry (Figure 12)

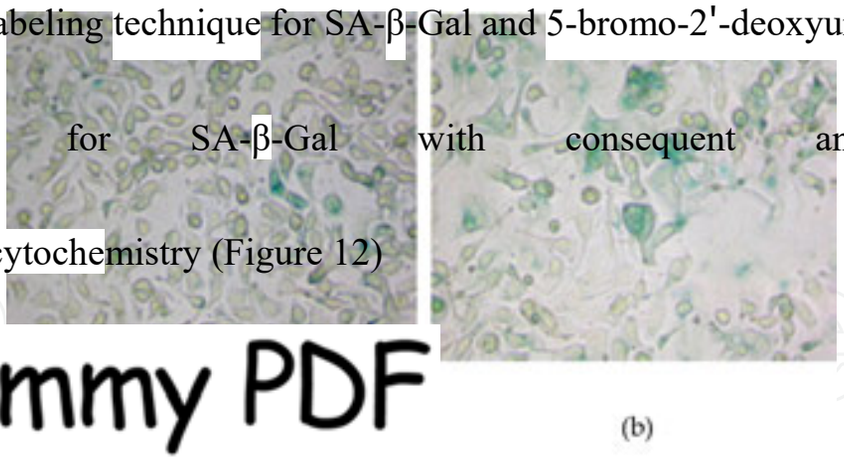

(b)

Figure 11. IR induces SLP associated with terminal growth arrest in human ATC cell lines: (a and c) non-irradiated; (b and d) in 120 hours after 10 Gy IR treatment; ATC cells exhibited typical features of SLP. Induction of SA-β-Gal activity (green) was mostly observed in large cells with increased granularity and flattened shape. SA-β-Gal staining method. (a) and (b) Bright-field microscopy, original magnification ×200. (c) and (d) Confocal fluorescent microscopy; original magnification ×400.

(green) was mostly observed in large cells with increased granularity and flattened shape. SA-β-Gal staining method. (a) and (b) Bright-field microscopy, original magnification ×200. (c) and (d) Confocal fluorescent microscopy; original magnification ×400.

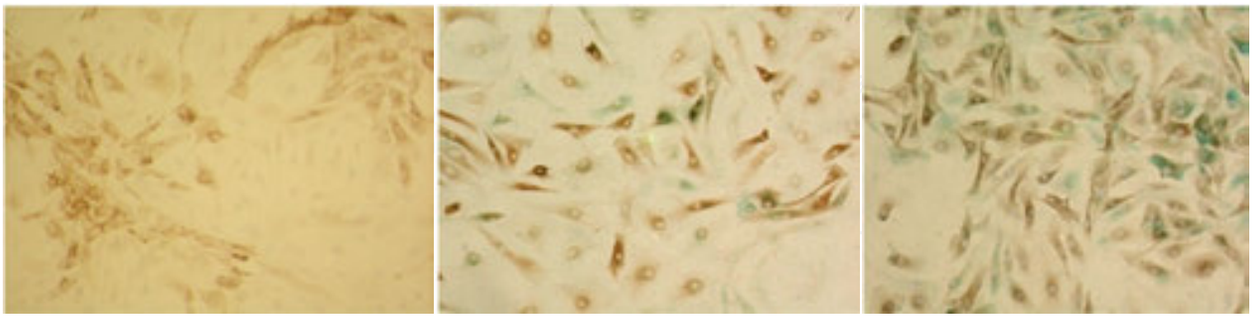

(a) (b) (c)

Figure 12. IR-induced SA-β-Gal activity in the primary culture of human thyroid follicular cells: (a) thyroglobulin-positive (brown) cells in primary culture, anti-thyroglobulin immunocytochemistry; (b) non-irradiated cells, double staining for SA-β-Gal and thyroglobulin; and (c) in 120 hours after 10 Gy IR treatment, double staining for SA-β-Gal and thyroglobulin. Original magnification ×200.

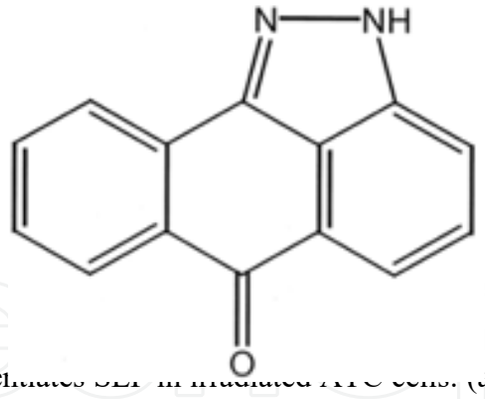

Figure 13. Chemical structure of anthrapyrazolone.

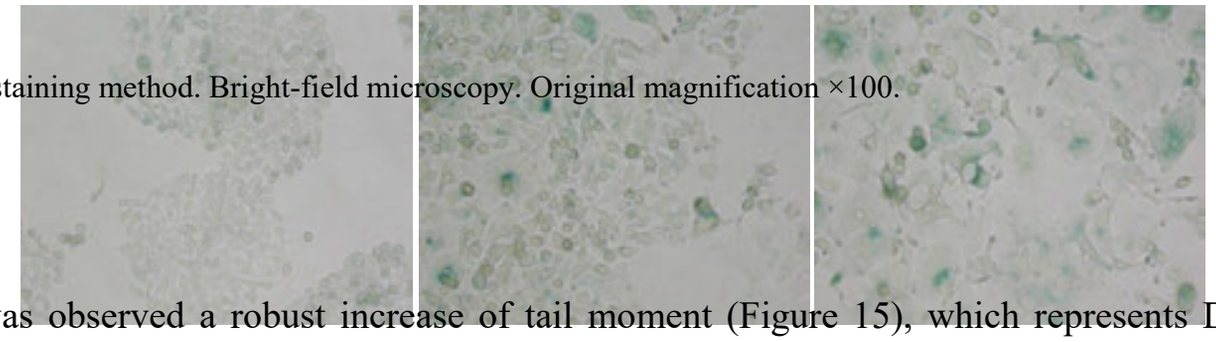

(a) (b) (c)

Figure 14. Anthrapyrazolone potentiates SLP in irradiated ATC cells: (a) non-radiated; (b) treatment with anthrapyrazolone; and (c) in 120 hours after 10 Gy IR treatment combined with anthrapyrazolone. SA-β-Gal staining method. Bright-field microscopy. Original magnification ×100.

It was observed a robust increase of tail moment (Figure 15), which represents DNA damage in alkaline single cell gel electrophoresis (Comet assay), in ATC cells treated with anthrapyrazolone plus IR compared to IR alone, suggesting that inhibition of JNK signaling pathway retarded DNA repair [7].

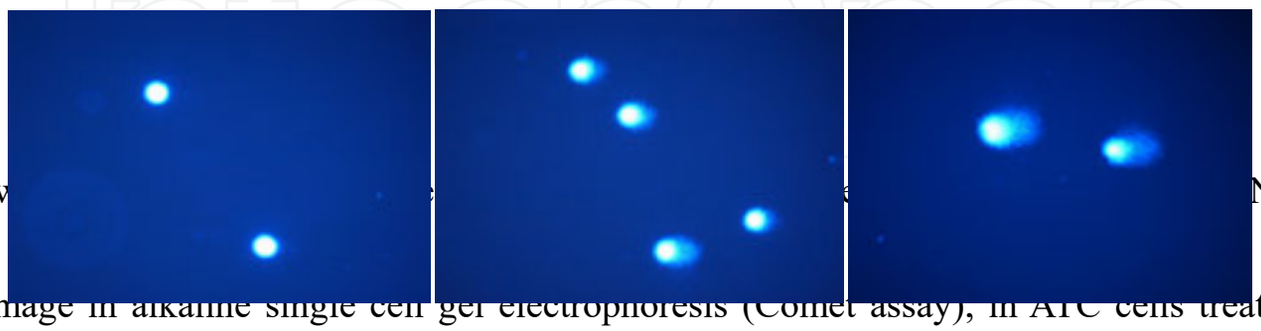

(a) (b) (c)

Figure 15. Anthrapyrazolone potentiates DNA damage in irradiated ATC cells: (a) non-radiated; (b) in 30 minutes after 10 Gy IR treatment; and (c) in 5 minutes after 10 Gy IR treatment combined with anthrapyrazolone. UV-fluorescent microscope.

In this study, DNA repair rates after 10 Gy exposure were analyzed by Comet assay to

In this study, DNA repair rates after 10 Gy exposure were analyzed by Comet assay to explore whether SLP induced by combination of anthrapyrazolone plus IR was associated with accumulation of DNA damage. In this method, individual cells with damaged DNA embedded in agarose gels are subjected to an electric field and generate a characteristic pattern of DNA distribution forming a tail that, after staining with fluorescence dye, can be analyzed by fluorescence microscopy. The extent and length of the comet's tail correlates with the severity of DNA damage [39].

Thus, one of the mechanisms that may contribute to the combination treatment effects is likely the delay of DNA repair evoked by JNK pathway inhibition. Treatment with anthrapyrazolone significantly delayed DNA rejoining after 10 Gy IR and increased the radiosensitivity of ATC cells.

7. Imatinib as a selective inhibitor of c-ABL tyrosine kinase activity

Imatinib (also known as STI571 or Gleevec®) is a tyrosine kinase inhibitor with selectivity toward BCR/ABL, c-ABL, platelet-derived growth factor receptor (PDGFR), and c-KIT (Figure 16) [40].

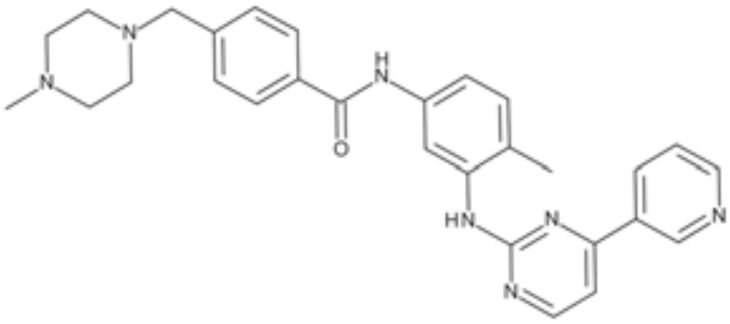

Figure 16. Chemical structure of imatinib.

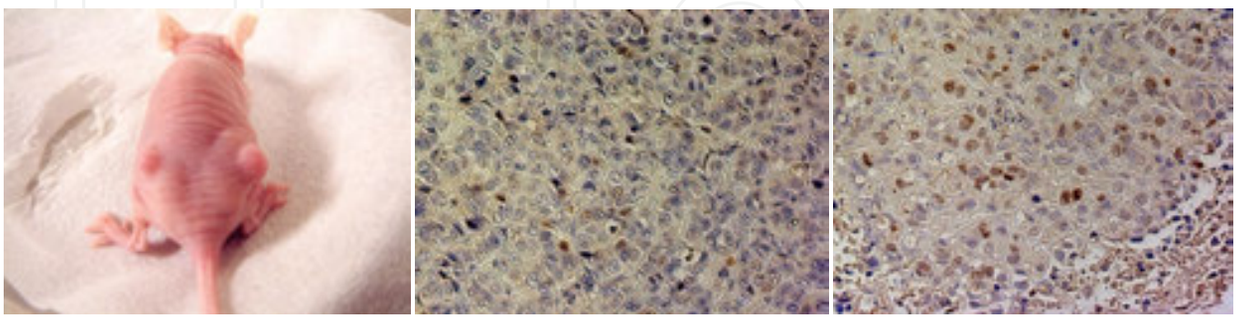

(a) (b) (c)

Figure 17. (a) ATC xenograft model (ATC cells were implanted s.c. into male athymic mice); (b) cell cycle inhibitor $p21^{cip1}$ expression in non-radiated mouse ATC cells xenograft; (c) imatinib 10 μM combined with single dose of 10 Gy IR in 120 hours after treatment. Imatinib suppressed *in vivo* growth of ATC cells implanted into nude mice. (b and c) immunohistochemistry, antibodies used were anti-$p21^{cip1}$. Original magnification ×200.

Figure 17. (a) ATC xenograft model (ATC cells were implanted s.c. into male athymic mice); (b) cell cycle inhibitor $p21^{cip1}$ expression in non-radiated mouse ATC cells xenograft; (c) imatinib 10 μM combined with single dose of 10 Gy IR in 120 hours after treatment. Imatinib suppressed *in vivo* growth of ATC cells implanted into nude mice. (b and c) immunohistochemistry, antibodies used were anti-

http://dx.doi.org/10.5772/62541

combined with single dose of 10 Gy IR in 120 hours after treatment. Imatinib suppressed *in vivo* growth of ATC cells implanted into nude mice. (b and c) immunohistochemistry, antibodies used were anti-$p21^{cip1}$. Original magnification ×200.

Imatinib impedes the growth of ATC cell lines *in vitro* through selective inhibition of c-ABL tyrosine kinase activity [41]. *In vivo*, imatinib combined with IR promotes $p21^{cip1}$ expression in mice bearing ATC xenograft model (Figure 17).

It was demonstrated that imatinib-induced S- and G2–M cell cycle arrest, leading to cell growth inhibition (Figure 18) [41].

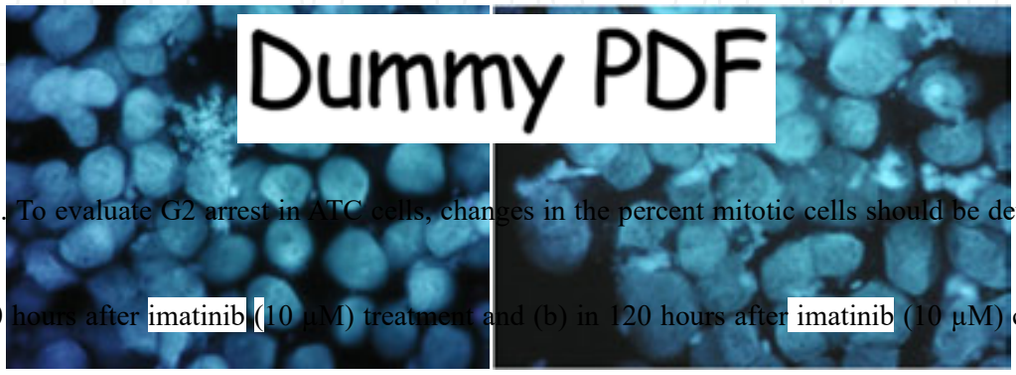

Figure 18. To evaluate G2 arrest in ATC cells, changes in the percent mitotic cells should be determined: (a) in 120 hours after imatinib (10 μM) treatment and (b) in 120 hours after imatinib (10 μM) combined with single dose of 5 Gy IR treatment.

The anti-tumor effect of imatinib is potentiated in adjunctive therapy with IR, not only due to inhibition of proliferative cell growth with transient cell cycle arrest and apoptosis but also due to the terminal growth arrest associated with SLP (Figure 19) [41].

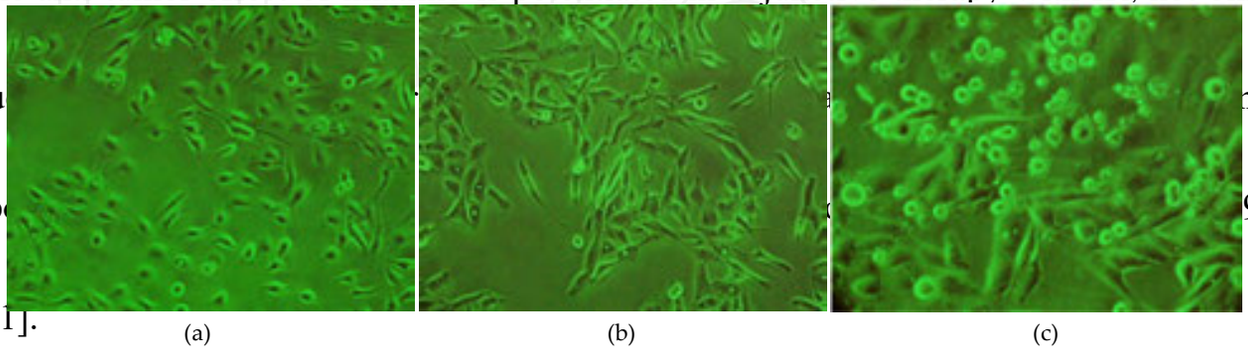

Figure 19. Phenotypic changes associated with SLP in ATC cells: (a) ATC cell line without treatment; (b) in 72 hours after imatinib (10 μM) treatment; (c) in 72 hours after imatinib (10 μM) treatment combined with single dose of 5 Gy IR. Enlarged and flattened morphology and increased granularity of ATC cells. Original magnification ×200.

16

8. Conclusion

Intracellular JNK and c-ABL signaling pathways are essential components of ATC cell proliferation and survival after radiation therapy. Hence, pharmacological inhibition of these pathways in combination with radiotherapy may be a potential treatment modality of ATC.

Author details

Dmitry Bulgin[1*] and Alexey Podcheko[2]

*Address all correspondence to: molmed1999@yahoo.com

1 Center for Regenerative Medicine "ME-DENT", Rovinj, Croatia

2 American University of Integrative Sciences, St. Maarten School of Medicine, Sint Maarten, Caribbean Netherlands

References

[1] Ain KB. Anaplastic thyroid carcinoma: behavior, biology, and therapeutic approaches. Thyroid 1998;8:715–726. DOI:10.1089/thy.1998.8.715

[2] Namba H, Hara T, Tukazaki T, *et al.* Radiation-induced G1 arrest is selectively mediated by the p53-WAF1/Cip1 pathway in human thyroid cells. Cancer Res. 1995;55:2075–2080.

[3] Yang T, Namba H, Hara T, *et al.* p53 induced by ionizing radiation mediates DNA end-jointing activity, but not apoptosis of thyroid cells. Oncogene 1997;14:1511–1519.

[4] Heron DE, Karimpour S, Grigsby PW. Anaplastic thyroid carcinoma: comparison of conventional radiotherapy and hyperfractionation chemoradiotherapy in two groups. Am J Clin Oncol. 2002;25:442–446.

[5] Harari PM, Huang SM. Modulation of molecular targets to enhance radiation. Clin Cancer Res. 2000;6:323–325.

[6] Bianco C, Bianco R, Tortora G, *et al*. Antitumor activity of combined treatment of human cancer cells with ionizing radiation and anti-epidermal growth factor receptor monoclonal antibody C225 plus type I protein kinase A antisense oligonucleotide. Clin Cancer Res. 2000;6:4343–4350.

[7] Bulgin D, Podtcheko A, Takakura S, *et al*. Selective pharmacologic inhibition of c-Jun NH2-terminal kinase radiosensitizes thyroid anaplastic cancer cell lines via induction of terminal growth arrest. Thyroid 2006;16:217–224. DOI:10.1089/thy.2006.16.217

[8] Verheij M. Clinical biomarkers and imaging for radiotherapy-induced cell death. Cancer Metastasis Rev. 2008;27:471–480. DOI:10.1007/s10555-008-9131-1

[9] Baskar R, Lee KA, Yeo R, Yeoh KW. Cancer and radiation therapy: current advances and future directions. Int J Med Sci. 2012;9:193–199. DOI:10.7150/ijms.3635

[10] Rogakou EP, Pilch DR, Orr AH, Ivanova VS, Bonner WM. DNA double-stranded breaks induce histone H2AX phosphorylation on serine 139. J Biol Chem. 1998;273:5858–5868. DOI:10.1074/jbc.273.10.5858

[11] Podhorecka M, Skladanowski A, Bozko P. H2AX phosphorylation: its role in DNA damage response and cancer therapy. J Nucl Acids. 2010;2010:920161. DOI: 10.4061/2010/920161

[12] Huang X, Halicka HD, Traganos F, Tanaka T, Kurose A, Darzynkiewicz Z. Cytometric assessment of DNA damage in relation to cell cycle phase and apoptosis. Cell Proliferat. 2005;38:223–243. DOI:10.1111/j.1365-2184.2005.00344.x

[13] Darzynkiewicz Z, Huang X, Okafuji M. Detection of DNA strand breaks by flow and laser scanning cytometry in studies of apoptosis and cell proliferation (DNA replication). Methods Mol Biol. 2006;314:81–93. DOI:10.1385/1-59259-973-7:081

[14] Eriksson D, Stigbrand T. Radiation-induced cell death mechanisms. Tumour Biol. 2010;31:363–372. DOI:10.1007/S13277-010-0042-8

[15] Hibi M, Lin A, Smeal T, Minden A, Karin M. Identification of an oncoprotein- and UV-responsive protein kinase that binds and potentiates the c-Jun activation domain. Genes Dev. 1993;7:2135–2148. DOI:10.1101/gad.7.11.2135

[16] Davis RJ. MAPKs: new JNK expands the group. Trends Biochem Sci. 1994;19:470–473.

[17] Prasad MV, Dermott JM, Heasley LE, *et al.* Activation of Jun kinase/stress-activated protein kinase by GTPase-deficient mutants of G alpha 12 and G alpha 13. J Biol Chem. 1995;270:18655–18659. DOI:10.1074/jbc.270.31.18655

[18] Westwick JK, Weitzel C, Minden A, *et al.* Tumor necrosis factor alpha stimulates AP-1 activity through prolonged activation of the c-Jun kinase. J Biol Chem. 1994;269:26396–26401.

[19] Cano E, Hazzalin CA, Mahadevan LC. Anisomycin-activated protein kinases p45 and p55 but not mitogen-activated protein kinases ERK-1 and -2 are implicated in the induction of c-fos and c-jun. Mol Cell Biol. 1994;14:7352–7362. DOI:10.1128/MCB.14.11.7352

[20] Watters D. Molecular mechanisms of ionizing radiation-induced apoptosis. Immunol Cell Biol. 1999;77:263–271. DOI:10.1046/J.1440-1711.1999.00824.X

[21] Kuwabara M, Takahashi K, Inanami O. Induction of apoptosis through the activation of SAPK/JNK followed by the expression of death receptor Fas in X-irradiated cells. J Radiat Res. 2003;44:203–209.

[22] Davis RJ. Signal transduction by the JNK group of MAP kinases. Cell 2000;103:239–252. DOI:10.1016/S0092-8674(00)00116-1

[23] Van Etten R.A. Cycling, stressed-out and nervous: cellular functions of c-ABL. Trends Cell Biol. 1999;9:179–186. DOI:10.1016/S0962-8924(99)01549-4

[24] Greuber EK, Smith-Pearson P, Wang J, Pendergast AM. Role of ABL family kinases in cancer: from leukaemia to solid tumours. Nat Rev Cancer. 2013;13:559–571. DOI: 10.1038/nrc3563

[25] Cheng L, Lloyd RV, Weaver AL, *et al.* The cell cycle inhibitors p21WAF1 and p27KIP1 are associated with survival in patients treated by salvage prostatectomy after radiation therapy. Clin Cancer Res. 2000;6:1896–1899.

[26] Yoshida K, Miki Y. Enabling death by the ABL tyrosine kinase: mechanisms for nuclear shuttling of c-ABL in response to DNA damage. Cell Cycle 2005;4:777–779.

[27] Shafman T, Khanna KK, Kedar P, *et al.* Interaction between ATM protein and c-ABL in response to DNA damage. Nature 1997;387:520–523. DOI:10.1038/387520a0

[28] Podtcheko A, Ohtsuru A, Namba H, *et al.* Inhibition of ABL tyrosine kinase potentiates radiation-induced terminal growth arrest in anaplastic thyroid cancer cells. Radiat Res. 2006;165:35–42.

[29] Yuan ZM, Huang Y, Whang Y, *et al.* Role for c-ABL tyrosine kinase in growth arrest response to DNA damage. Nature 1996;382:272–274. DOI:10.1038/382272a0

[30] Sionov RV, Moallem E, Berger M, *et al*. c-ABL neutralizes the inhibitory effect of Mdm2 on p53. J Biol Chem. 1999;274:8371–8374. DOI:10.1074/jbc.274.13.8371

[31] Ito T, Seyama T, Mizuno T, *et al.* Unique association of p53 mutations with undifferentiated but not with differentiated carcinomas of the thyroid gland. Cancer Res. 1992;52:1369–1371.

[32] Fagin JA, Matsuo K, Karmakar A, *et al.* High prevalence of mutations of the p53 gene in poorly differentiated human thyroid carcinomas. J Clin Invest. 1993;91:179–184. DOI:10.1172/JCI116168

[33] Namba H, Hara T, Tukazaki T, *et al.* Radiation-induced G1 arrest is selectively mediated by the p53-WAF1/Cip1 pathway in human thyroid cells. Cancer Res. 1995;55:2075–2080.

[34] Whang YE, Tran C, Henderson C, *et al*. c-ABL is required for development and optimal cell proliferation in the context of p53 deficiency. Proc Natl Acad Sci USA. 2000;97:5486–5491.

[35] Schmitt CA. Cellular senescence and cancer treatment. Biochim Biophys Acta. 2007;1775:5–20. DOI:10.1016/j.bbcan.2006.08.005

[36] Podtcheko A, Namba H, Saenko V, *et al.* Radiation-induced senescence-like terminal growth arrest in thyroid cells. Thyroid 2005;15:306–313. DOI:10.1089/thy.2005.15.306

[37] Bennett BL, Sasaki DT, Murray BW, *et al*. SP600125, an anthrapyrazolone inhibitor of Jun N-terminal kinase. Proc Natl Acad Sci USA. 2001;98:13681–13686. DOI:10.1073/pnas.251194298

[38] Gururajan M, Chui R, Karuppannan AK, *et al.* c-Jun N-terminal kinase (JNK) is required for survival and proliferation of B-lymphoma cells. Blood 2005;106:1382–1391. DOI:10.1182/blood-2004-10-3819

[39] Ostling O, Johanson KJ. Microelectrophoretic study of radiation-induced DNA damages in individual mammalian cells. Biochem Biophys Res Commun. 1984;123:291–298. DOI:10.1016/0006-291X(84)90411-X

[40] Krystal GW, Honsawek S, Litz J, Buchdunger E. The selective tyrosine kinase inhibitor STI571 inhibits small cell lung cancer growth. Clin Cancer Res. 2000;6:3319–3326.

[41] Podtcheko A, Ohtsuru A, Tsuda S, *et al.* The selective tyrosine kinase inhibitor, STI571, inhibits growth of anaplastic thyroid cancer cells. J Clin Endocrinol Metab. 2003;88:1889–1896. DOI:10.1210/jc.2002-021230

IntechOpen